

Focus Evaluation Approach for Retinal Images

Diana Veiga^{1,2}, Carla Pereira¹, Manuel Ferreira^{1,2}, Luís Gonçalves³ and João Monteiro²

¹ENERMETER, Parque Industrial Celeirós 2ª Fase, Lugar de Gaião, Lotes 5/6, 4705-025 Braga, Portugal

²Centro Algoritmi, University of Minho, Azurém, 4800-058 Guimarães, Portugal

³Oftalmocenter, Rua Francisco Ribeiro de Castro, nº 205, Azurém, 4800-045 Guimarães, Portugal

Keywords: Digital Fundus Photography, Focus Measures, Image Processing.

Abstract: Digital fundus photographs are often used to provide clinical diagnostic information about several pathologies such as diabetes, glaucoma, macular degeneration and vascular and neurologic disorders. To allow a precise analysis, digital fundus image quality should be assessed to evaluate if minimum requirements are present. Focus is one of the causes of low image quality. This paper describes a method that automatically classifies fundus images as focused or defocused. Various focus measures described in literature were tested and included in a feature vector for the classification step. A neural network classifier was used. HEI-MED and MESSIDOR image sets were utilized in the training and testing phase, respectively. All images were correctly classified by the proposed algorithm.

1 INTRODUCTION

Eye fundus imaging allows the observation of the retina and the analysis of its constituents. With this medical imaging examination several pathologies can be diagnosed, mainly those related with blood vessels modifications. In recent years there have been numerous research attempts for the development of systems to automatically analyze fundus images. The success of these systems is frequently affected by image quality which sometimes is poor due to bad acquisition conditions or the presence of occlusions, cataracts and opacities in patients' eyes. For a proper automated analysis, fundus images must present a minimum quality that not always is possible to guarantee by clinicians in the capturing moment. Focus is one of the parameters responsible for a reduced quality image, which we propose to verify in digital fundus photography.

The task of eye fundus image acquisition demands a specific training as numerous conditions must be fulfilled. Moreover, despite some commercial fundus cameras comprise tools to assist the photographer in the operation, focusing on the fundus can be difficult and subjective.

Focus measures appear as methods to estimate the sharpness of an image. Various algorithms have

been proposed for auto-focusing, estimating depth, or just to determine the degree of blurring (Marrugo, 2012); (Yap, 2004); (Yang, 2003); (Pertuz, 2013) (Moscaritolo, 2009). Pertuz et al., (2013) divides the most popular measures in different groups: Gradient-based operators, Wavelet-based operators, Statistic-based operators, DCT-based operators and Miscellaneous operators. However, very few of these methods have been tested in fundus images (Marrugo, 2012).

In general, a single focus operator is applied to an image. Nonetheless, since fundus images content extremely varies, a single focus operator cannot always achieve a correctly focus estimation. To address this issue, in this work, a group of focus measures were selected and combined to be used in a neural network classifier. A new approach to automatically classify retinal images as focused/defocused is described. Several experiments were carried out using real focused fundus images and synthetically defocused ones. Numerous focus operators were tested and applied on the referred digital images and their response to blur was evaluated. In addition, this study reports the application of an artificial neural network classifier to obtain the final classification of retinal images. Three focus measures were considered as input features to the classifier: a wavelet-based measure, a

moment-based measure and a third measure based on a statistic operator.

The paper is organized in the following sections: Section 2 defines the methodology of the proposed approach presenting the focus measures selected and the neural network classifier. Also the datasets of retinal images used in the experiments are detailed in this section. Results are demonstrated and discussed in Section 3. Finally, conclusions and future work are addressed in section 4.

2 METHODOLOGY

The proposed approach aims to classify an eye fundus image as focused or defocused after its acquisition by the expert. The classifier inputs result from the application of different focus operators. In order to have a reasonable focus measure, some pre-requisites must be complied: the obtained value should decrease as blur augments; it should be content-independent and robust to noise.

2.1 Eye Fundus Images

The Hamilton Eye Institute Macular Edema Dataset (HEI-MED) (Giancardo, 2012) and the MESSIDOR database were used to test the focus measures and the implemented classifier. HEI-MED contains 169 fundus images of different patients, with a reasonable mixture of ethnicities and disease state. MESSIDOR database is comprised by 1200 images, but only 200 were utilized.

Fundus images were artificially degraded to achieve a defocused image from a focused one. The degradation process operates on an input image $f(x,y)$, where a degradation function $h(x,y)$ together with additive noise $\eta(x,y)$ produce a degraded image $g(x,y)$. If $\eta(x,y) = 0$, it yields the expression

$$g(x,y) = f(x,y) * h(x,y) \quad (1)$$

The symbol $*$ refers to convolution. The 2-D Gaussian function was used as degradation function to produce the blurring effect. This function is named point spread function (PSF) since this will blur (spread) a point of light to some degree, with the amount of blurring being determined by the kernel size of 30×30 , 50×50 and standard deviation $\sigma = 5, 15, 30, 45$. Other size masks were tested but only these were chosen to be shown here as they are representative in terms of initial visual detection of the blurring effect and distortion of the image.

The training set consists of 200 images, 100

randomly chosen from the HEI-MED dataset and the same images defocused. The test set is composed by 200 images, 100 original images and another 100 degraded with blur, from MESSIDOR. Figure 1 show three example images focused and defocused from HEI-MED and MESSIDOR dataset.

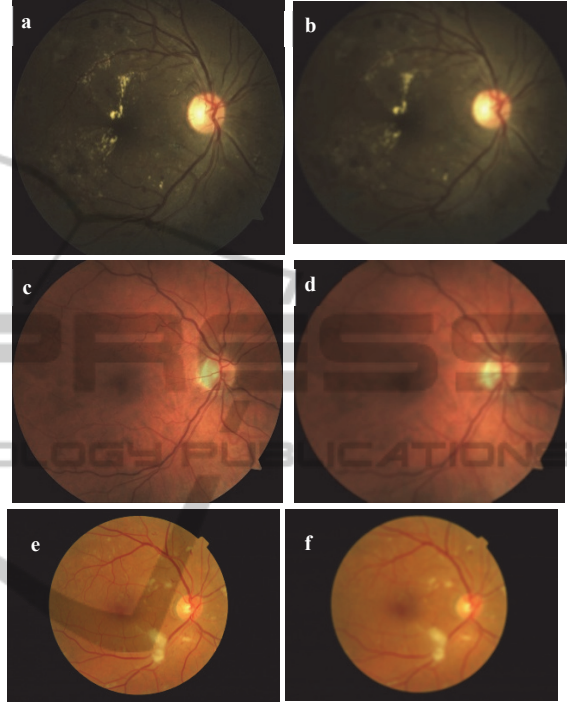


Figure 1: Digital fundus photographs from HEI-MED and MESSIDOR. a) and c) Original image from HEI-MED; b) and d) image a) and c) artificially defocused, respectively; e) original image from MESSIDOR; f) artificially defocused image from MESSIDOR. All defocused images were obtained with kernel 30×30 and $\sigma=45$.

2.2 Wavelet-based Focus Measure

The focus measure operator utilized has been proposed by Yang et al., (2003) and is constructed in the wavelet transform domain. Wavelets measure functional intensity variations along different directions: horizontal (columns), vertical (rows) and diagonal. A schematic representation of the wavelet decomposition is depicted in Figure 2.

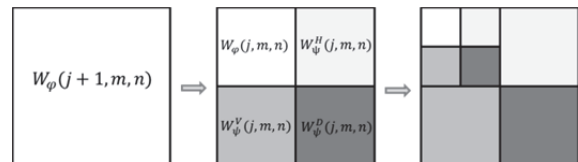


Figure 2: The 2-D Wavelet transform decomposition level j , along m rows and n columns.

The focus measure operator is defined as the mean value of sum of detail coefficients of wavelets decompositions in the first level, as follows (Yang, 2003):

$$FM_{wt}^1 = \frac{1}{mn} \sum_m \sum_n [|W_{\psi}^H(1, m, n)| + |W_{\psi}^V(1, m, n)| + |W_{\psi}^D(1, m, n)|] \quad (2)$$

Here, the Daubechies Db6 mother wavelet was used in the first level of decomposition, following the same conditions as in (Yang, 2003). This measure reflects the high-frequency component of the image, which results from the high-pass filters of the discrete wavelet transform. It is possible to perceive that as blur increases the high-frequency information contained in the image will decrease, making this operator a good metric to evaluate focus.

2.3 Moment-based Focus Measure

Orthogonal moments have been used in many applications such as image analysis, pattern recognition, image segmentation, edge detection, image registration among others. Their success is due to their low information redundancy, capacity of object description, invariance properties, information compactness and transmission of spatial and phase information of an image (Papakostas, 2009); (Wee, 2010). The most well-known orthogonal moments are the Zernike and Legendre moments. Chebyshev moments differ from the previous as they are discrete orthogonal moments.

Inspired by the studies of Raveendran *et al.* (Yap, 2004); (Wee, 2010), an image focus measure based on Chebyshev moments was developed. Different computation strategies appear to accelerate these moments computation (Papakostas, 2009). Here, the recursive strategy was followed to calculate the Chebyshev polynomials, as in (Wee, 2010),

$$(p + 1) t_{p+1}(x) = (2p + 1)(2x - M + 1) t_p(x) - p(M^2 - p^2) t_{p-1}(x) \quad (3)$$

Where the order p is $p = 1, \dots, M - 1$, and the Chebyshev polynomials of zero and first order are $t_0(x) = 1$ and $t_1(x) = 1 - M + 2x$, respectively.

In 2-dimensional images of size $M \times N$, Chebyshev moments of order $p + q$ behave as a filterbank, where the convolution of a kernel defined by the Chebyshev polynomials, with the image will retain the image information. Figure 2 displays the basis images (kernels) for the 2-dimensional discrete Chebyshev moments until the 4th order (2+2).

After performing the convolution with the obtained kernels, the maximum intensity value of each 8×8 non-overlapping square region was computed and the average for each order moment was subsequently determined. The matrix $M(x,y)$ shows the moments organization,

$$M(x, y) = \begin{bmatrix} M_{00} & M_{01} & M_{02} \\ M_{10} & M_{11} & M_{12} \\ M_{20} & M_{21} & M_{22} \end{bmatrix} \quad (4)$$



Figure 3: Basis images of low-order Chebyshev moments.

The final focus measure is calculated as the ratio between the summed values for moments of order $p + q > 1$ and $p + q \leq 1$,

$$FM_{CM} = \frac{M_{11} + M_{12} + M_{20} + M_{21} + M_{22} + M_{02}}{M_{00} + M_{01} + M_{10}} \quad (5)$$

2.4 Statistical-based Focus Measure

The last focus measure applied to extract image content information uses a median filter and calculates the mean energy of the resulting image.

The median filter is normally used in preprocessing steps of fundus images analysis algorithms to reduce noise. This filter outperforms the mean filter since it preserves useful details of the image. The difference is that the median filter considers the nearby neighbors to decide whether or not a central pixel is representative of its surroundings and replaces it with the median of those values. By subtraction of the filtered image to the original green plane image a difference image with enhanced edges is obtained, $Idif(x,y)$.

The statistics-based focus measure, FM_{med} , is calculated using the following expression,

$$FM_{med} = \sum_x \sum_y Idif(x,y)^2 \quad (6)$$

This focus measure explores the fact that in a sharp image, edges will appear with increased definition than in blurred images. Consequently, the energy of the former will be higher than the latter.

2.5 Artificial Neural Network (ANN) Classifier

Neural networks are powerful computational tools that attempt to mimic the brain function. Similarly to the brain, artificial neural networks comprise neurons organized in several layers. Different types of ANN are described in literature and the selection task of the most adequate is not an easy one.

Here, a multi-layer neural network with one hidden layer constituted by 20 neurons was constructed. The number of neurons was experimentally tested. As hidden neuron activation function the hyperbolic tangent sigmoid transfer function was used. In the output layer, we used the logistic sigmoid activation function, which is also a sigmoidal function defined in [0, 1].

In this work, the classifier purpose is to classify digital fundus photographs as focused or defocused, for which we attribute classes 1 and 0, respectively. The input vector for the neural network consists of a three dimensional feature vector, corresponding to the focus measures scores for each image. Three focus measures were developed and added to the classifier input features.

For the training phase the developed network used backpropagation algorithm with the mean square error function to enhance its performance.

3 RESULTS & DISCUSSION

In this section, the results of the applied focus measures and the neural network classifier outputs are presented.

First, the focus measures were tested independently on the original focused and artificially blurred images of the HEI-MED dataset. Different kernel sizes (30×30 , 40×40 , 50×50) and standard deviations were used to blur the images. The Gaussian function was employed as the PSF. All focus measures were computed in the green plane of the RGB fundus images. A mask of the field of view was determined and applied to only investigate the retina content. Figures 4, 5 and 6 show the measurements results of focus by varying

the standard deviation of five images of the selected image database. The defocused images analyzed were obtained with the kernel of size 30×30 . Figure 4 regards to the wavelet-based focus measure, Figure 5 to the moment-based approach and Figure 6 to the statistics-base method.

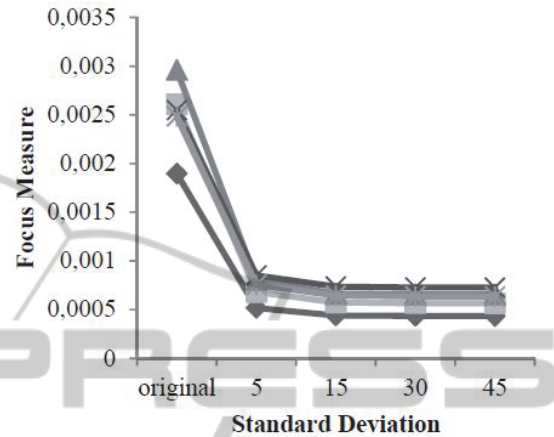


Figure 4: Wavelet-based focus measure.

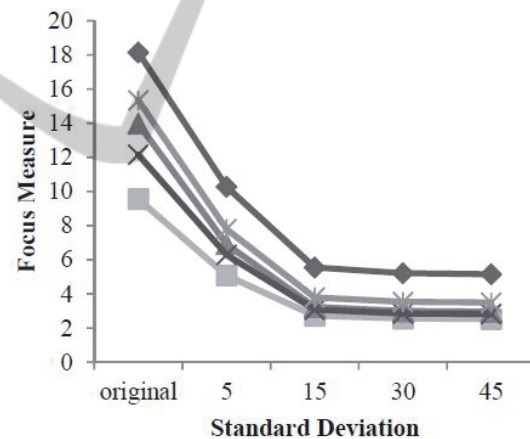


Figure 5: Basis images of low-order Chebyshev moments.

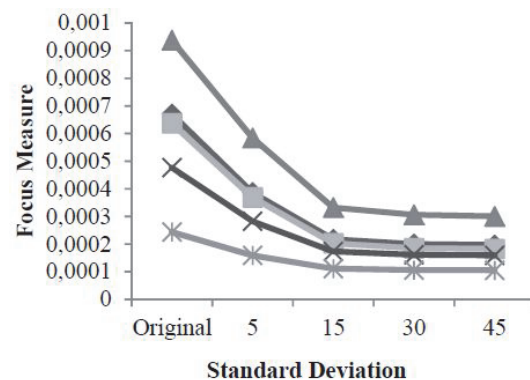


Figure 6: Basis images of statistic-based focus measure.

It is possible to observe in Figures 4, 5 and 6 that the focus measures are monotonically decreasing, that is, as blur augments the focus operators output value become lower. In the case of the wavelet-based operator (Figure 4), the focus measure has a larger decrease from the original image to the blurred one with $\sigma=5$. However, the decline is less accentuated between the different defocused scales. In the moment-based and statistics-based operators (Figure 5 and 6), the focus value decreases between the original and $\sigma=15$ defocused image, remaining almost equal for further blurring degree. This behavior was observed in the entire set of images. It is also important to note that even within the set of original focused images, the measured value of focus varies widely. Nonetheless, the value always decreases when blur is present.

To make our approach more robust and flexible in terms of the eye fundus content diversity, a group of focus measures were combined to form the input vector of a classifier. The classifier adds robustness to the developed approach since it contours the pitfalls of each method individually. A feedforward backpropagation neural network was constructed to the classification phase of the fundus images regarding focus. The training was conducted with 100 images randomly chosen of the HEI-MED dataset and 100 images artificially blurred. Next, the network was tested with 200 images from the MESSIDOR database.

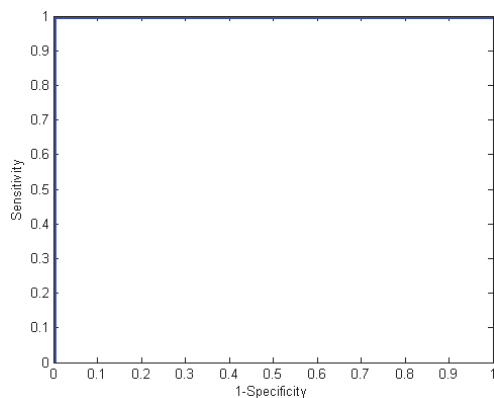


Figure 7: ROC curve of the test images (MESSIDOR) classification.

The output of the classifier comprises only two classes: 1-focused, and 0-defocused. Matlab was used to produce the ROC curve and calculate the AUC (area under curve). ROC curves plot the true positive fraction (or sensitivity) versus the false positive fraction (or one minus specificity). Here, sensitivity refers to the ability to classify an image correctly as focused when it really is focused and

specificity is the number of defocused images classified as focused. It was obtained an optimal ROC curve with 100 % sensitivity and specificity with all images correctly classified (Figure 7). The AUC was consequently 1.

4 CONCLUSIONS

A new focus measure approach was presented in this paper. It is based on focus operators that were never tested in fundus images. The moment-based focus measure was adapted from literature and the statistics-based operator was developed and added to increase the approach robustness. All operators were tested independently. Due to the variability of fundus images, a combined approach that could embrace these variances and surpass the focus measures handicaps was developed. Blurred images were correctly identified among a heterogeneous group of focused and defocused images.

Results are promising and further images should be tested. As future work, we expect to gather original defocused images to test the proposed method. Also, it is expected to combine this technique with another that identifies the presence of bright artifacts originated in the acquisition moment by illumination. Other classifiers will also be tested in order to compare performance.

Image quality evaluation of fundus images is an important task that should precede the diagnosis by an automatic system. The proposed focus method can be an essential part of such a system.

ACKNOWLEDGEMENTS

Work supported by FEDER funds through the “Programa Operacional Factores de Competitividade – COMPETE” and by national funds by FCT – Fundação para a Ciência e a Tecnologia. D. Veiga thank the FCT for the SFRH/BDE/51824/2012.

MESSIDOR images were kindly provided by the MESSIDOR program partners.

REFERENCES

- Giancardo, L. et al., 2012. Exudate-based diabetic macular edema detection in fundus images using publicly available datasets. *Medical image analysis*, 16(1), pp.216–26.
- Marrugo, A.G. et al., 2012. Anisotropy-based robust focus measure for non-mydratric retinal imaging. *Journal of*

- biomedical optics*, 17(7), p.076021.
- Moscaritolo, M. et al., 2009. An image based auto-focusing algorithm for digital fundus photography. *IEEE transactions on medical imaging*, 28(11), pp.1703–7.
- Papakostas, G. A., Mertzios, B.G. & Karras, D. a., 2009. Performance of the Orthogonal Moments in Reconstructing Biomedical Images. *2009 16th International Conference on Systems, Signals and Image Processing*, pp.1–4.
- Papakostas, G. & Koulouriotis, D., 2009. A General Framework for Computation of Biomedical Image Moments. *Biomedical Engineering Trends in Electronics, Communications and Software*.
- Pertuz, S., Puig, D. & Garcia, M. A., 2013. Analysis of focus measure operators for shape-from-focus. *Pattern Recognition*, 46(5), pp.1415–1432.
- Wee, C.-Y. et al., 2010. Image quality assessment by discrete orthogonal moments. *Pattern Recognition*, 43(12), pp.4055–4068.
- Yang, G. & Nelson, B., 2003. Wavelet-based autofocusing and unsupervised segmentation of microscopic images. *International Conference on Intelligent Robots and Systems, Proceedings of the 2003 IEEE/RSJ*, (October).
- Yap, P. T. & Raveendran, P., 2004. Image focus measure based on Chebyshev moments. *IEEE Proc.-Vision, Image and Signal Processing*, 151(2).